Journal of Physical Research: Biogeosciences

Supporting Information for

Exorcizing Divergence in Tree-Ring Density along the Rocky Mountains

Marcel Kunz[1], Max C.A. Torbenson[2,3], Frederick Reinig[1], Edurne Martinez del Castillo[1], Ulf Büntgen[3,4,5], Rob Wilson[6,7], Inga K. Homfeld[1], Greg King[8], Emily Reid[6], Kevin J. Anchukaitis[7,9,10], Valerie Trouet[9,10], Karen E. King[11], Grant L. Harley[12], Justin T. Maxwell[13], Adam Csank[14], Ellie Broadman[10], Eileen Kuhl[15], Julie Edwards[16], Philipp Römer[1], Björn Günther[17,18], Christian Gerber[18,19], Jan Esper[1,3]

[1]Department of Geography, Johannes Gutenberg University, 55128 Mainz, Germany

[2]Department of Geography, Texas A&M University, College Station, TX 77843, USA

[3]Global Change Research Institute of the Czech Academy of Sciences (CzechGlobe), 61300 Brno, Czech Republic

[4]Department of Geography, University of Cambridge, Cambridge CB2 3EN, UK

[5]Department of Geography, Faculty of Science, Masaryk University, Brno, Czech Republic

[6]School of Earth and Environmental Sciences, University of St. Andrews, St. Andrews KY16 9AJ, Scotland, UK

[7]Tree Ring Laboratory, Lamont-Doherty Earth Observatory, Palisades, NY 10964, USA

[8]Department of Science, University of Alberta Augustana Campus, Camrose, AB T4V 2R3, Canada

[9]School of Geography, Development, and Environment, University of Arizona, Tucson, AZ 85721, USA

[10]Laboratory of Tree-Ring Research, University of Arizona, Tucson, AZ 85721, USA

[11]Department of Geography and Sustainability, University of Tennessee, Knoxville, TN 37996, USA

[12]Department of Earth and Spatial Sciences, University of Idaho, Moscow, ID 83844, USA

[13]Department of Geography, Indiana University Bloomington, Bloomington, IN 47405, USA

[14]Department of Geography, University of Nevada, Reno, Reno, NV 89557, USA

[15]Deutscher Wetterdienst (German Meteorological Service), 63067 Offenbach, Germany

[16]Bren School of Environmental Science & Management, Santa Barbara, CA 93117, USA

[17]Chair of Soil Resources and Land Use, Institute of Soil Science and Site Ecology, Dresden University of Technology, 01737 Tharandt, Germany

[18]Core Facility Environmental Analytics (CFEA), Dresden University of Technology, 01737 Tharandt, Germany

[19]Chair of Forest Utilization, Institute of Forest Utilization and Technology, Dresden University of Technology, 01737 Tharandt, Germany

Contents of this file

Introduction

This file includes three different types of supporting information:

1. Figures and a table that provide additional information on the sampling sites.
2. Individual plots for each individual site, that were summarized in one single plot for main figures 2, 3, and 5.
3. Figures that support the conclusions drawn in the Discussion section by providing more specific additional information and analyses.

Figure S1. Sampling sites along the Rocky Mountains with **(a)** Mancha Creek, **(b)** Twelvemile Summit, **(c)** North Klondike River, **(d)** Canyon Lake, **(e)** Pink Mountain, **(f)** Sunwapta, **(g)** Baker Lake, **(h)** Pikes Peak, and **(i)** Mount Belknap.

Table S1 (next page). Sampling sites along the Rocky Mountains with site coordinates, elevation, monthly mean temperature and precipitation estimates based on nearest 0.5° x 0.5° CRU TS 4.08 grid cell (Harris et al. 2020) for Alaska and Canada and nearest PRISM 4km grid cell (Daly et al. 1994) for the contiguous US, as well as covered period and corresponding sites used in Briffa et al. (1998) with site coordinates, elevation, distance to Monostar site, and covered period. Information marked with * is based on data taken from the ITRDB and likely inaccurate.

MONOSTAR site	Mancha Creek	Twelvemile Summit	North Klondike River	Canyon Lake	Pink Mountain	Sunwapta	Baker Lake	Pikes Peak	Mount Belknap
Code	MAC	TWE	NKL	CNY	PIN	SUN	BAK	PIK	BEL
Latitude	68.67	65.38	64.44	61.12	57.04	52.21	45.89	38.87	38.42
Longitude	-141.02	-145.95	-138.26	-136.99	-122.86	-117.22	-114.27	-105.07	-112.40
Elevation [m a.s.l.]	566	971	984	1108	1512	2051	2423	3583	3179
Jan Tmean [°C]	-29	-25	-29	-21	-15	-13	-8	-9	-7
Feb Tmean [°C]	-30	-22	-25	-17	-12	-10	-5	-9	-7
Mar Tmean [°C]	-26	-16	-16	-11	-7	-9	-3	-7	-5
Apr Tmean [°C]	-18	-6	-6	-3	1	-3	2	-3	-1
May Tmean [°C]	-6	4	4	4	7	2	6	1	4
Jun Tmean [°C]	3	11	10	9	12	6	11	6	9
Jul Tmean [°C]	7	13	12	11	14	8	15	10	13
Aug Tmean [°C]	5	10	9	9	12	8	15	8	12
Sep Tmean [°C]	-1	4	3	4	8	4	10	5	9
Oct Tmean [°C]	-12	-8	-7	-3	2	-1	4	1	3
Nov Tmean [°C]	-23	-19	-21	-14	-8	-9	-3	-6	-3
Dec Tmean [°C]	-26	-23	-27	-19	-14	-13	-7	-9	-7
Jan Prec [mm]	0-10	5-15	15-25	10-20	30-40	145-155	135-145	10-20	110-120
Feb Prec [mm]	0-10	5-15	15-25	5-15	25-35	110-120	95-105	20-30	130-140
Mar Prec [mm]	5-15	0-10	15-25	5-15	25-35	105-115	80-90	35-45	195-205
Apr Prec [mm]	0-10	0-10	15-25	0-10	20-30	65-75	5-15	55-65	150-160
May Prec [mm]	0-10	10-20	15-25	5-15	45-55	55-65	75-85	65-75	60-70
Jun Prec [mm]	20-30	40-50	40-50	30-40	65-75	90-100	65-75	55-65	25-35
Jul Prec [mm]	25-35	45-55	50-60	40-50	80-90	85-95	30-40	105-115	45-55
Aug Prec [mm]	30-40	35-45	45-55	30-40	55-65	70-80	35-45	125-135	75-85
Sep Prec [mm]	5-15	10-20	25-35	5-15	40-50	70-80	50-60	45-55	55-65
Oct Prec [mm]	0-10	0-10	15-25	0-10	25-35	80-90	65-75	30-40	70-80
Nov Prec [mm]	0-10	0-10	20-30	5-15	30-40	120-130	85-95	40-50	120-130
Dec Prec [mm]	0-10	5-15	20-30	5-15	30-40	125-135	120-130	25-35	115-125
Period	1794-2021	1612-2021	1795-2021	1820-2021	1864-2022	1480-2021	1460-2020	1539-2021	1560-2021
Period n ≥ 5	1808-2021	1873-2021	1823-2021	1835-2021	1874-2022	1561-2021	1727-2020	1567-2021	1607-2021
Briffa et al. site	Northway Junction	Denali	Northway Junction	Don Jek River Bridge	Fort Nelson	Sunwapta Pass	Lost Trail Pass	Pike Peaks	Electric Lake
Latitude	62.83	63.67	62.83	61.67	58.33	52.25	45.7	39.33*	39.58*
Longitude	-141.33	-149.58	-141.33	-139.67	-122.83	-117	-113.95	-105.03*	-111.33*
Distance [km]	652	259	235	156	144	16	33	51*	160*
Elevation [m a.s.l.]	600	750	600	750	690	2000	2130	3600	2970
Period	1795-1983	1551-1983	1795-1983	1585-1983	1817-1983	1608-1983	1785-1983	1530-1983	1542-1983
Period n ≥ 5	1799-1983	1631-1983	1799-1983	1697-1983	1818-1983	1623-1983	1795-1983	1644-1983	1724-1983

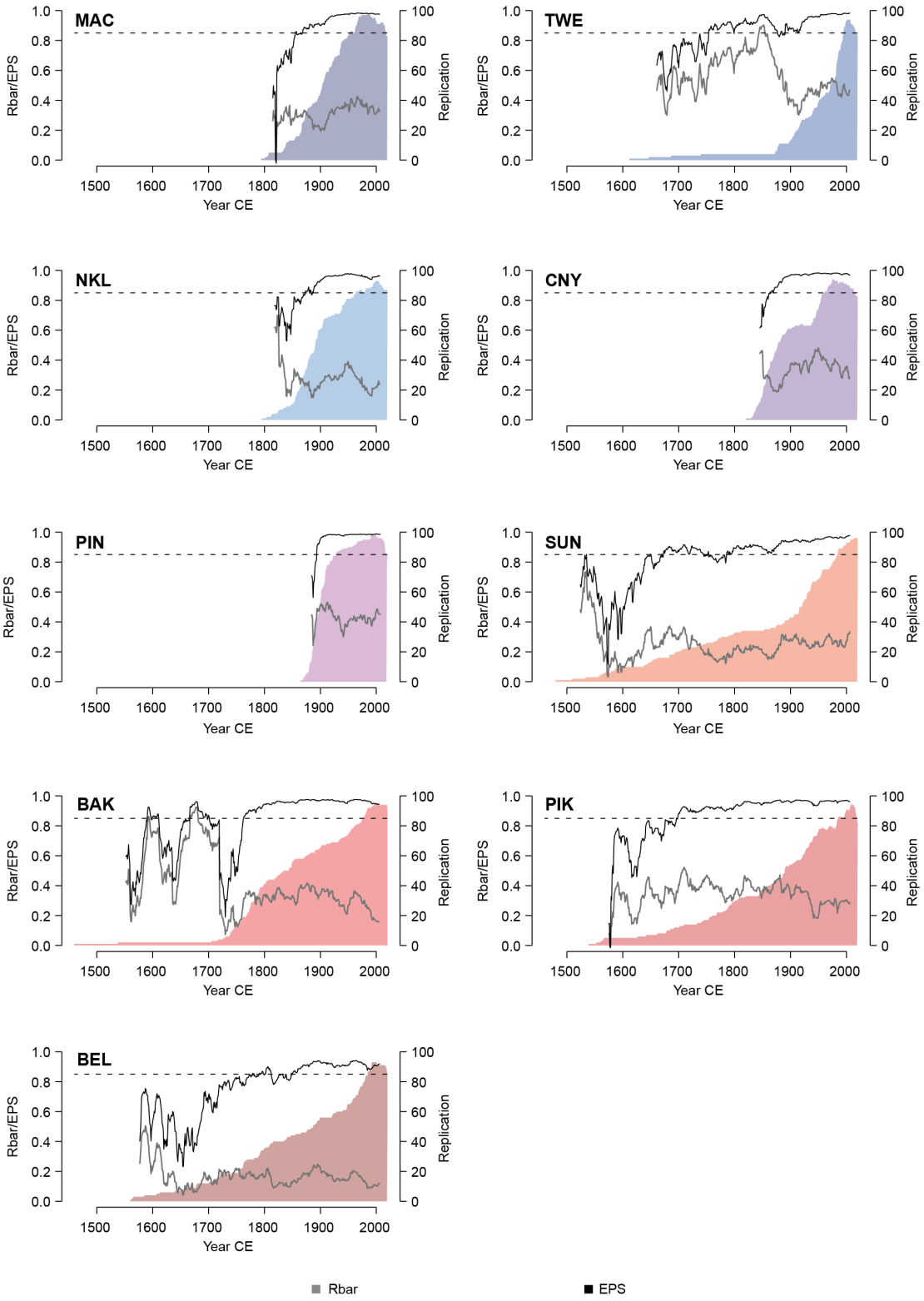

Figure S2. 31-year moving-window Rbar and EPS statistics as well as sample replication of MXD datasets. Dashed horizontal lines denote the widely accepted threshold of 0.85 for sufficient EPS.

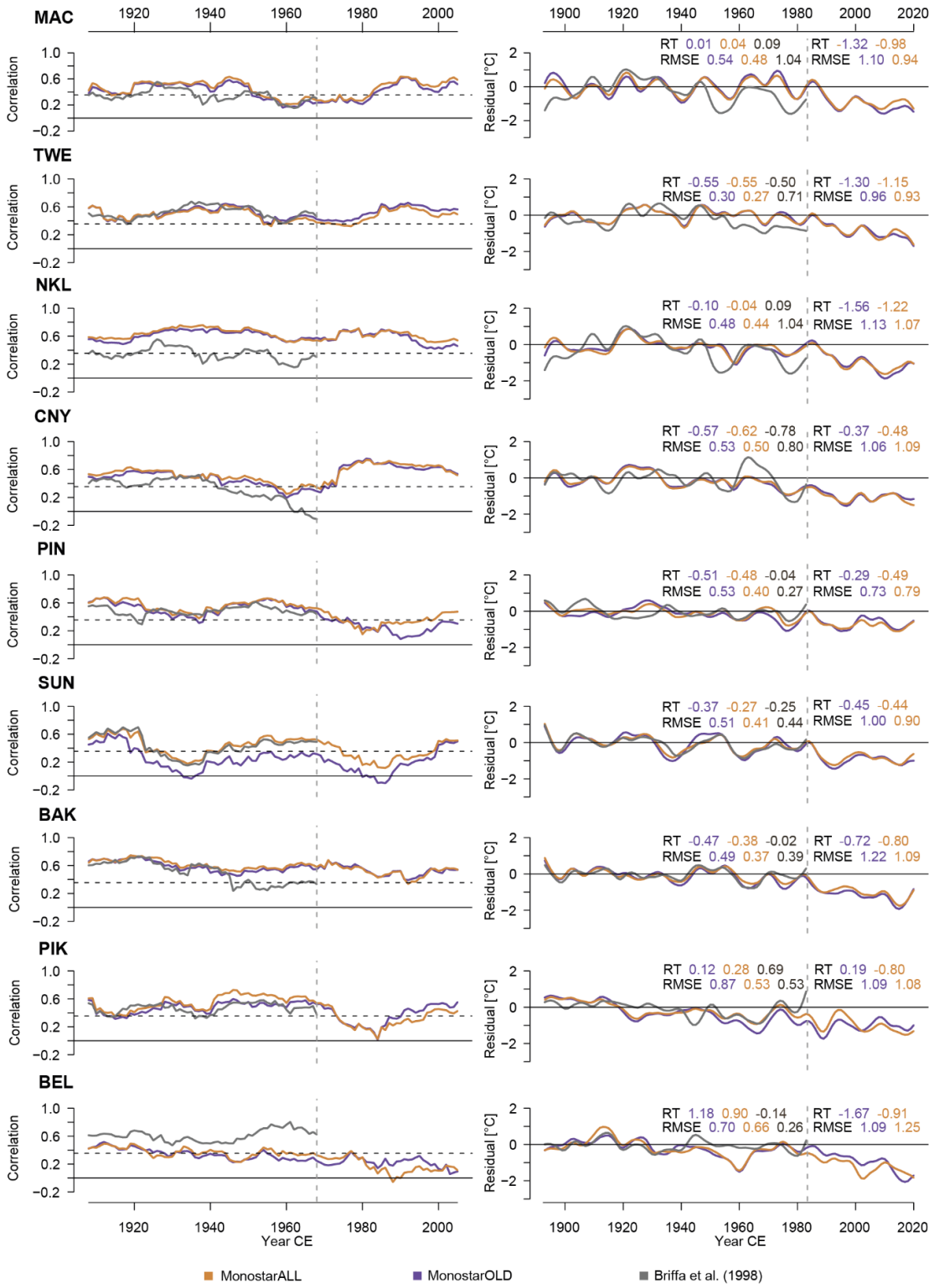

Figure S3. Centered 31-year moving correlations and 10-year low-pass filtered residual trends between scaled (1893–1950), Hugershoff detrended MXD MonostarALL, MonostarOLD, and Briffa et al. (1998) chronologies and Berkeley Earth mean temperatures for single sites. Numbers denote RMSE and linear residual trends (RT) in °C for the common period of all datasets (1951–1983) and the subsequent period until present (1984–2020). Vertical dashed lines indicate end years of the Briffa chronologies.

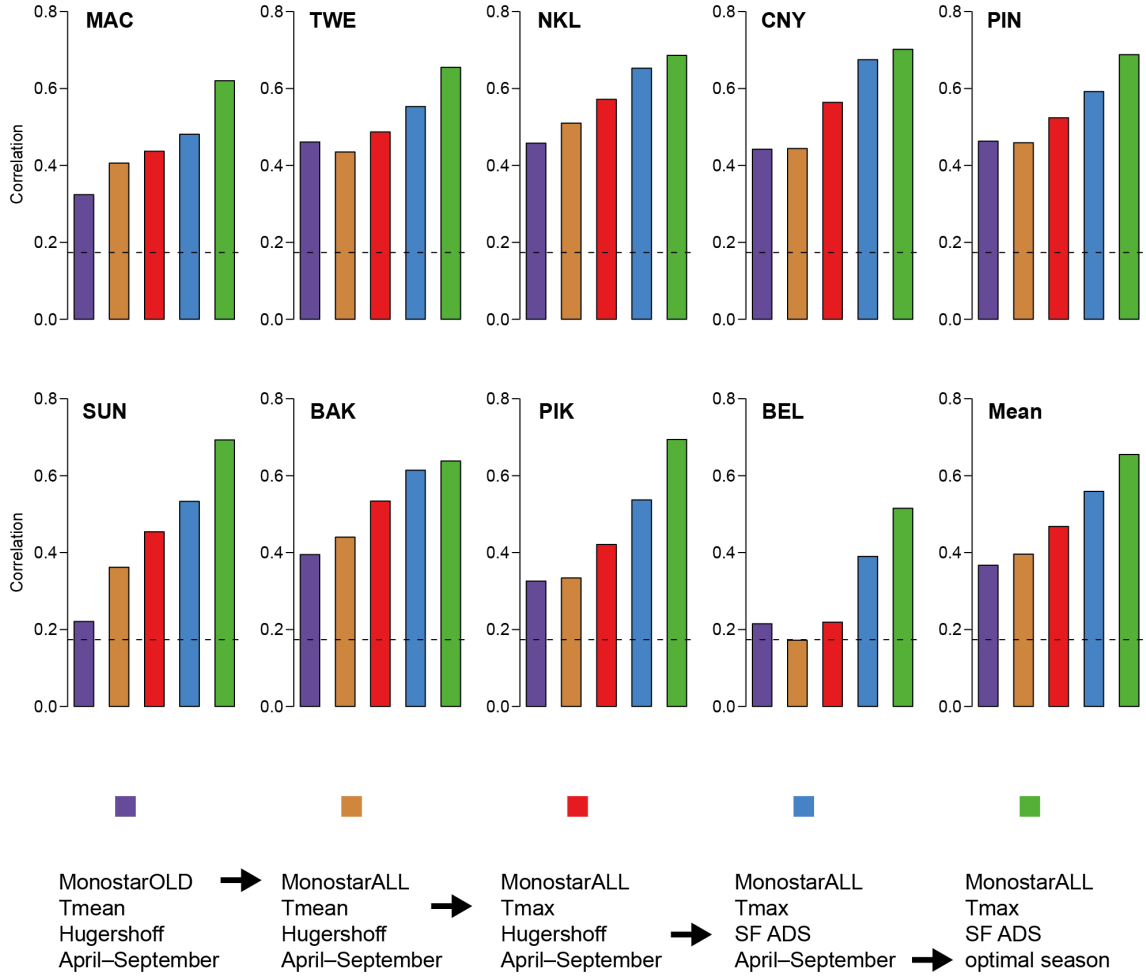

Figure S4. Stationary full-period (1893–2020) correlations for different combinations of MXD and instrumental data for single sites as well as the mean of all nine sites.

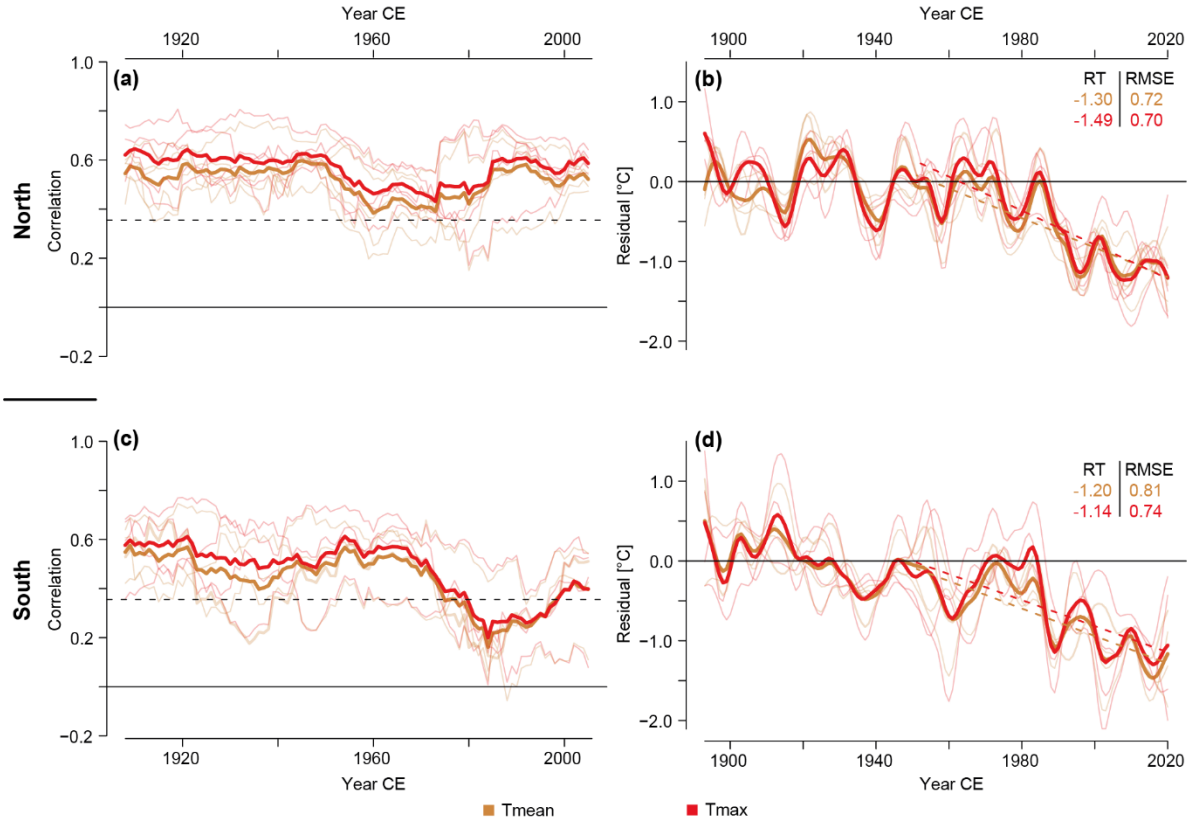

Figure S5. Centered 31-year moving correlations **(a, c)** and trends of 10-year smoothed residuals trends **(b, d)** calculated between regional April–September mean or maximum temperatures and Hugershoff detrended MXD chronologies. All chronologies were scaled from 1893–1950. Thin lines refer to single sites and solid lines to group means. RMSE and linear residual trends (RT) in °C are calculated over the 1951–2020 period.

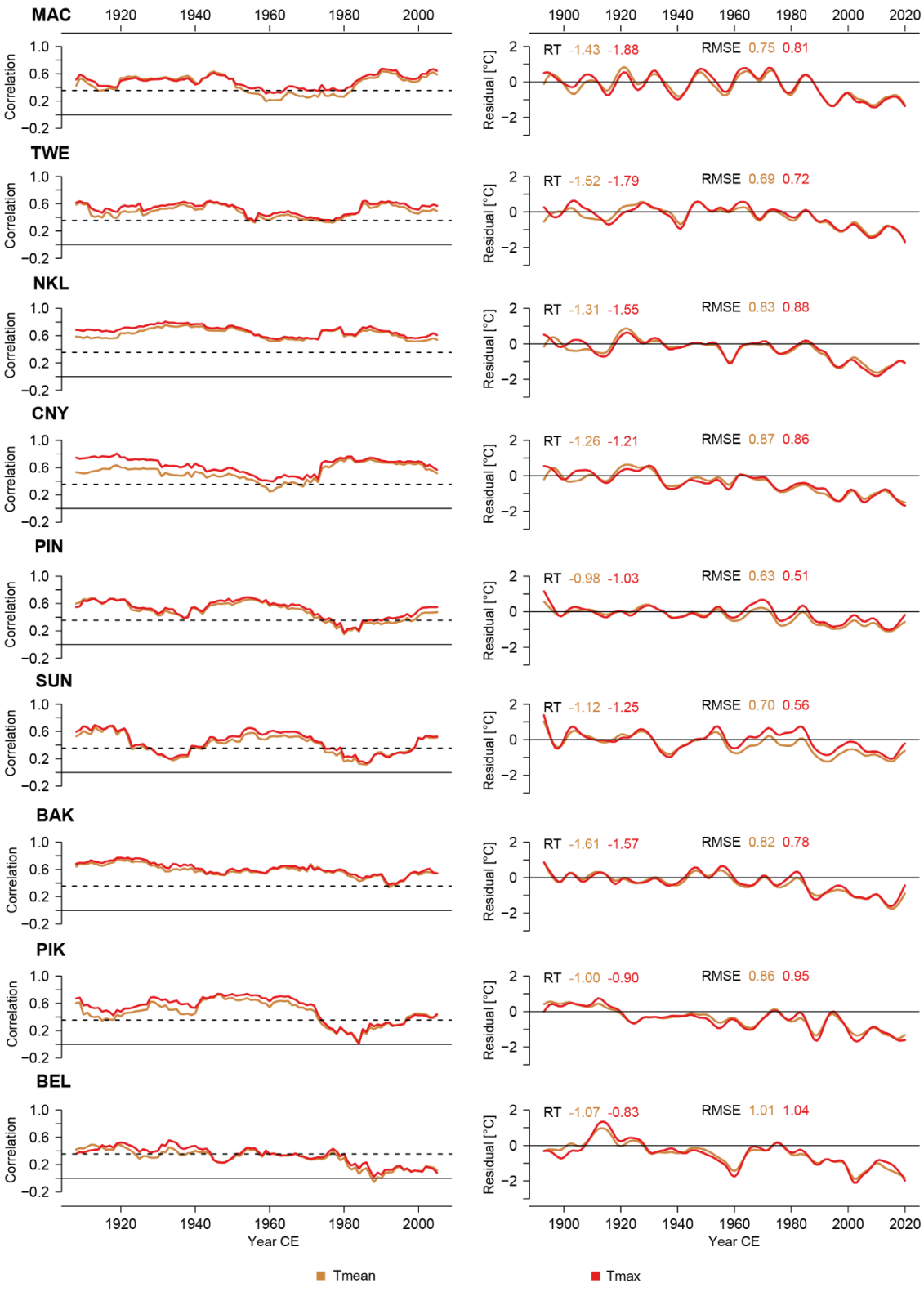

Figure S6. Centered 31-year moving correlations and 10-year low-pass filtered residual trends between scaled (1893–1950) MXD chronologies and BEST mean and maximum temperatures for single sites. Numbers denote RMSE and linear residual trends (RT) in °C for the 1951–2020 period.

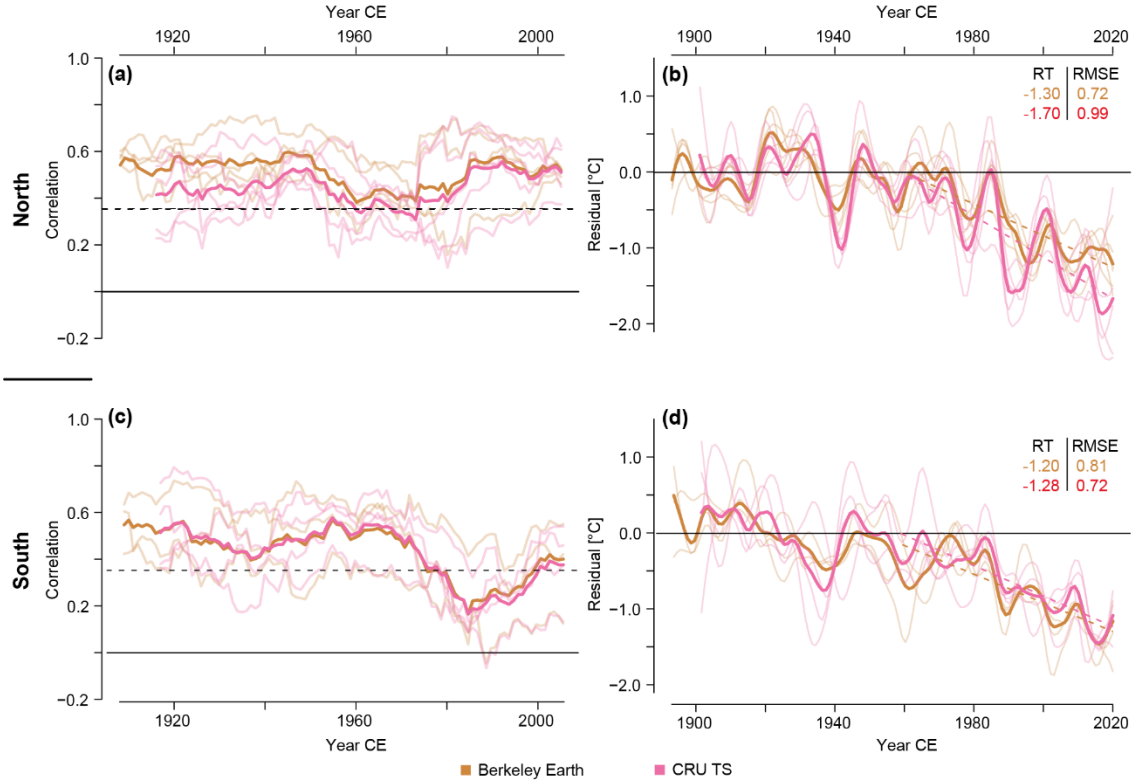

Figure S7. Centered 31-year moving correlations **(a, c)** and trends of 10-year smoothed residuals trends **(b, d)** calculated between regional April–September Berkeley Earth or CRU TS mean temperatures and Hugershoff detrended MXD chronologies. All chronologies were scaled from 1893–1950. Thin lines refer to single sites and solid lines to group means. RMSE and linear residual trends (RT) in °C are calculated over the 1951–2020 period.

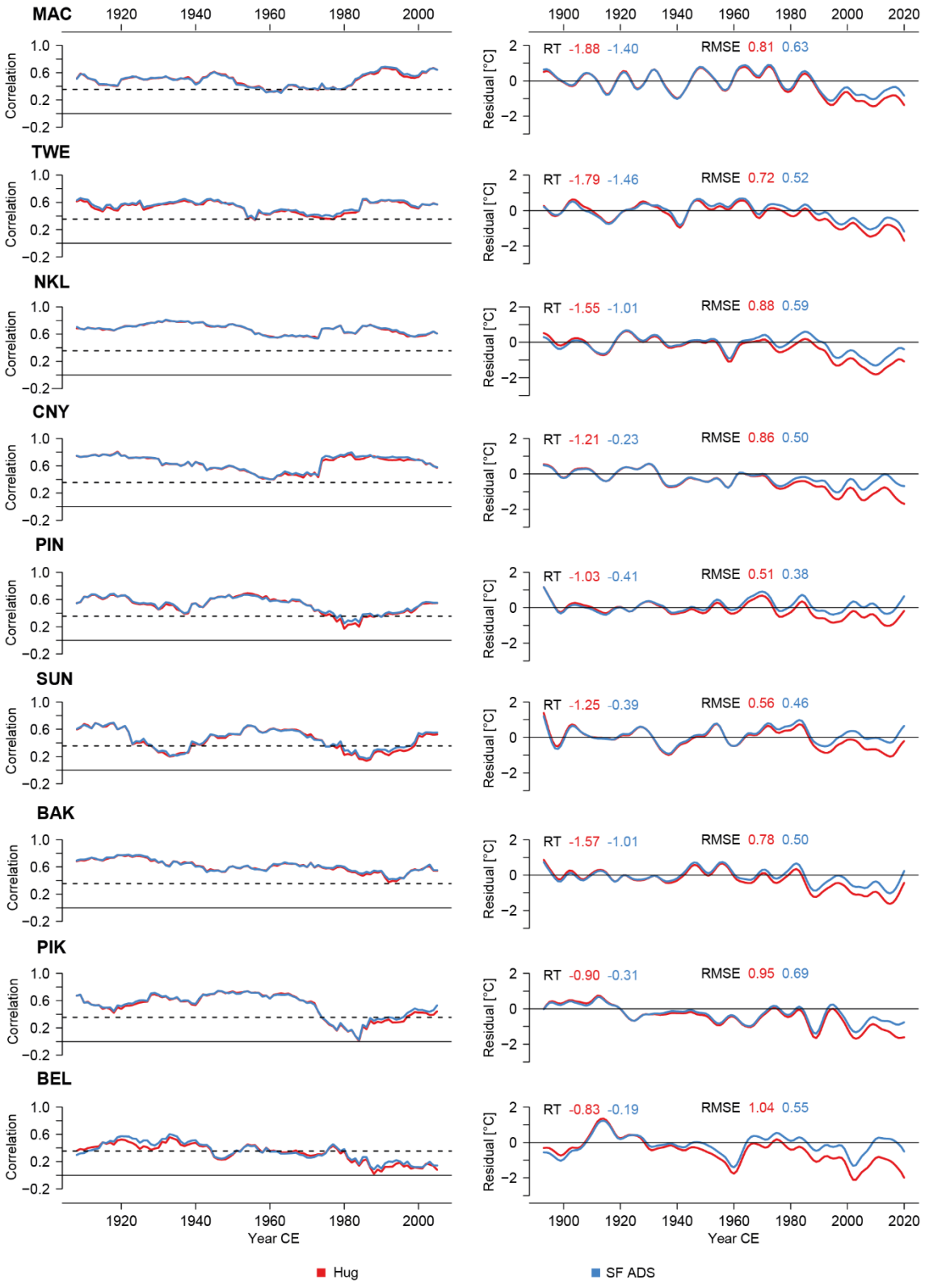

Figure S8. Centered 31-year moving correlations and 10-year low-pass filtered residual trends between scaled (1893–1950) Hugershoff (Hug) and signal-free age-dependent spline (SF ADS) detrended MXD chronologies and BEST maximum temperatures for single sites. Numbers denote RMSE and linear residual trends (RT) in °C for the 1951–2020 period.

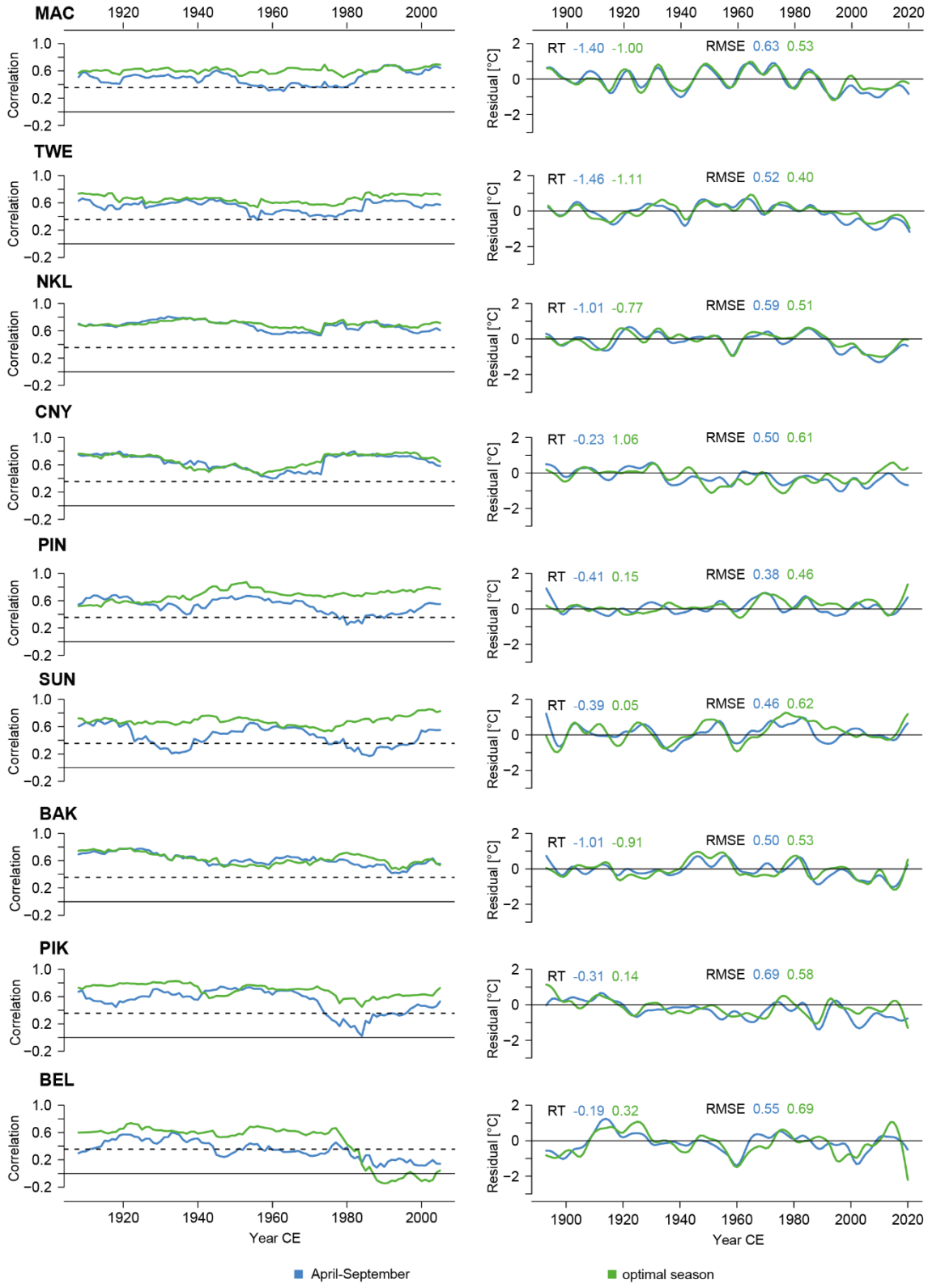

Figure S9. Centered 31-year moving correlations and 10-year low-pass filtered residual trends between scaled (1893–1950) signal-free age-dependent spline detrended MXD chronologies and April–September and optimal season BEST maximum temperatures for single sites. Numbers denote RMSE and linear residual trends (RT) in °C for the 1951–2020 period.

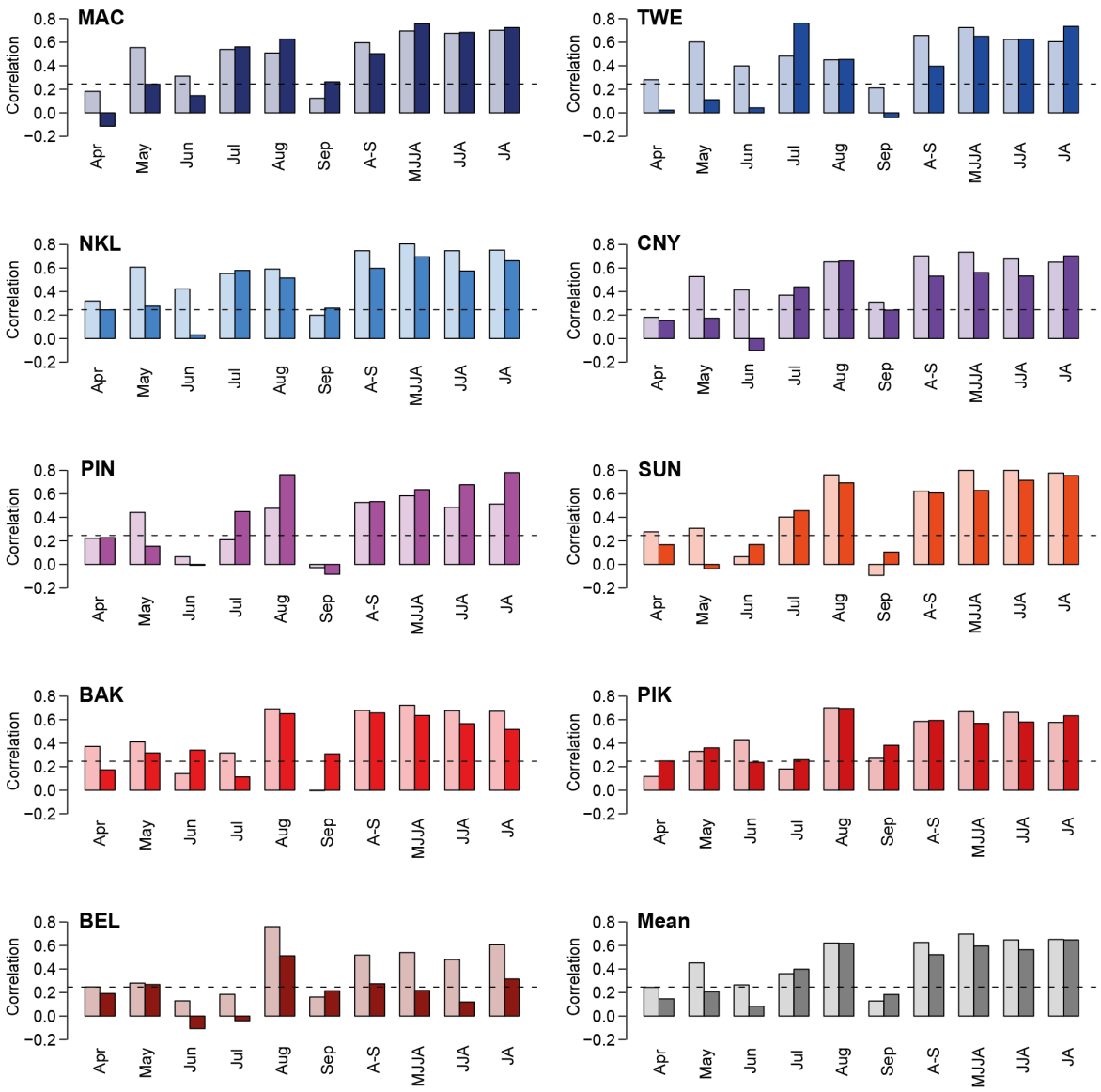

Figure S10. First-differenced correlations between signal-free age-dependent spline detrended MXD chronologies and Tmax for the first (1894–1957, light colors) and second half (1957–2020, dark colors) of the common period of tree-ring and instrumental data.

.

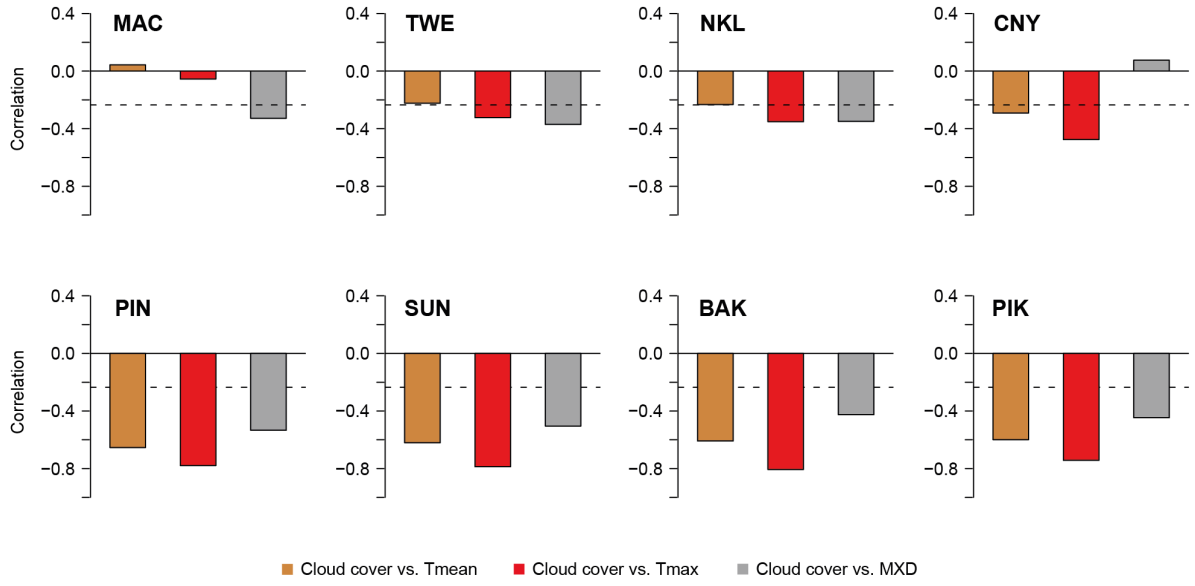

Figure S11. Full period (1894–2020) correlations between gridded April–September cloud cover and Tmean, Tmax, as well as MXD data for single sites. No usable cloud cover data was available for the BEL site.

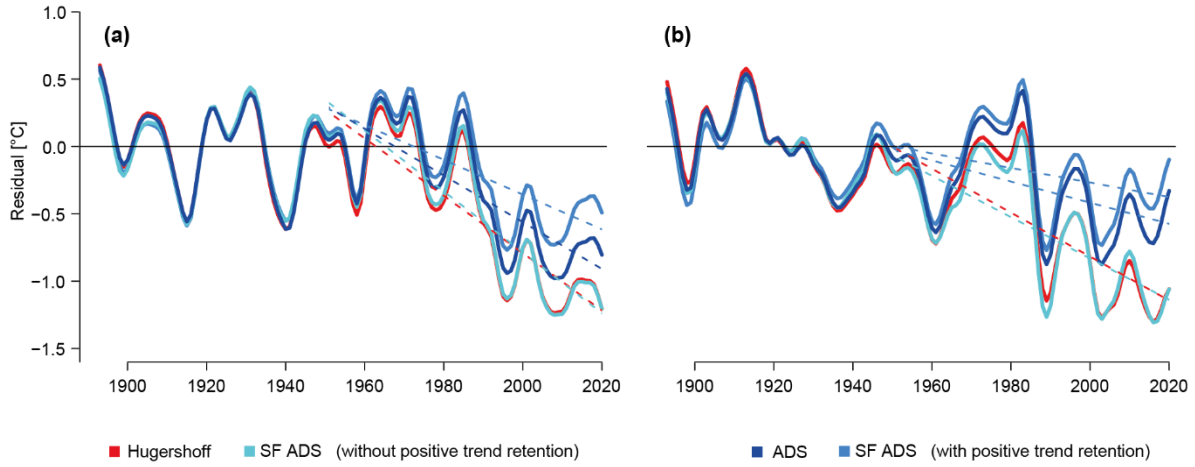

Figure S12. 10-year low-pass filtered residuals between scaled (1893–1950) Hugershoff (Hug) and age-dependent spline (ADS) as well as signal-free age-dependent spline (SF ADS, with and without positive trend retention) detrended MXD chronologies and BEST April–September maximum temperatures for the northern **(a)** and southern groups **(b)**. Dashed lines indicate linear residual trends for the 1951–2020 period.

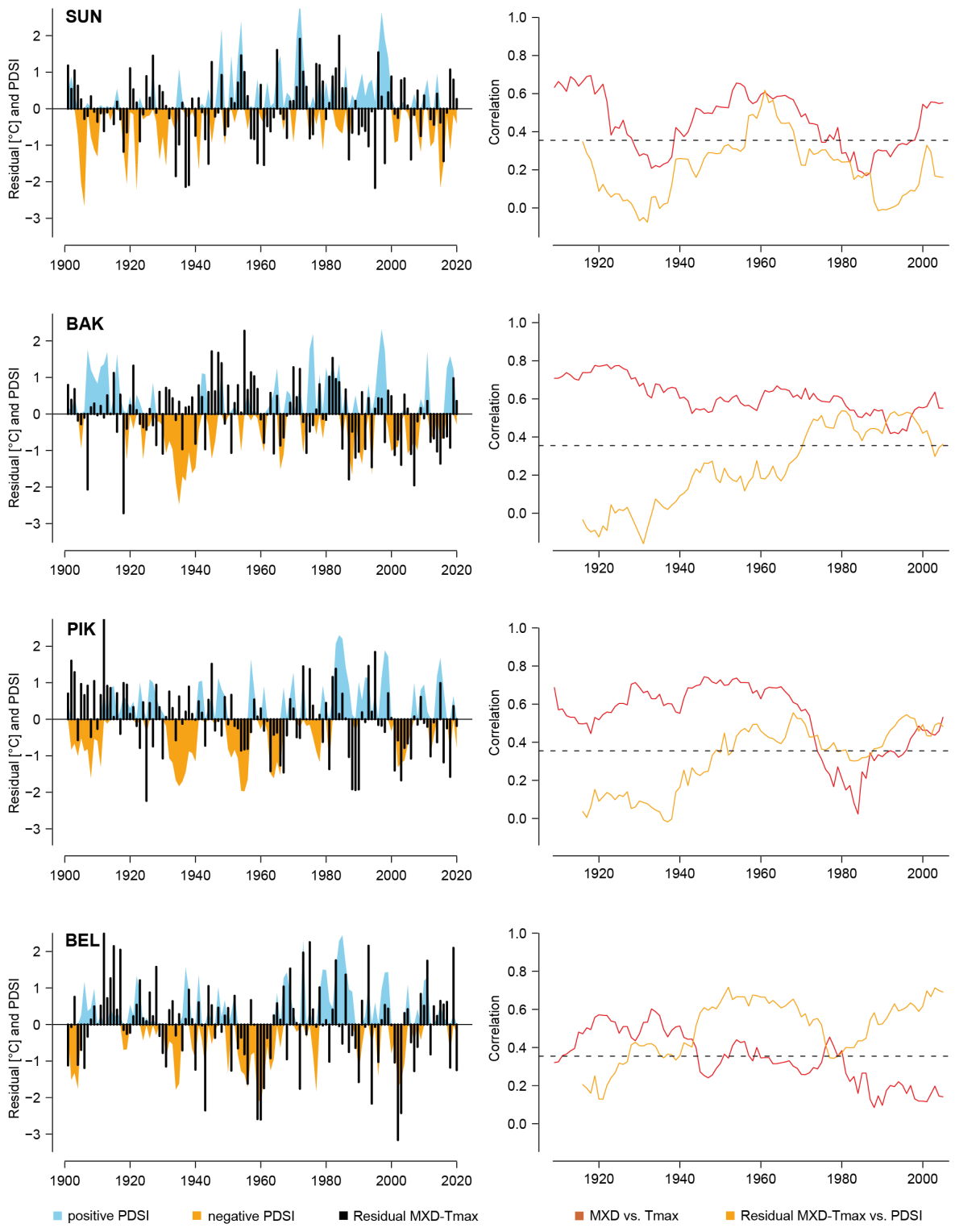

Figure S13. Effect of drought on MXD temperature signals of southern sites with MXD-Tmax residuals (black bars) and PDSI (colored areas) as well as centered 31-year moving correlations between MXD and Tmax and between MXD-Tmax residuals and PDSI.

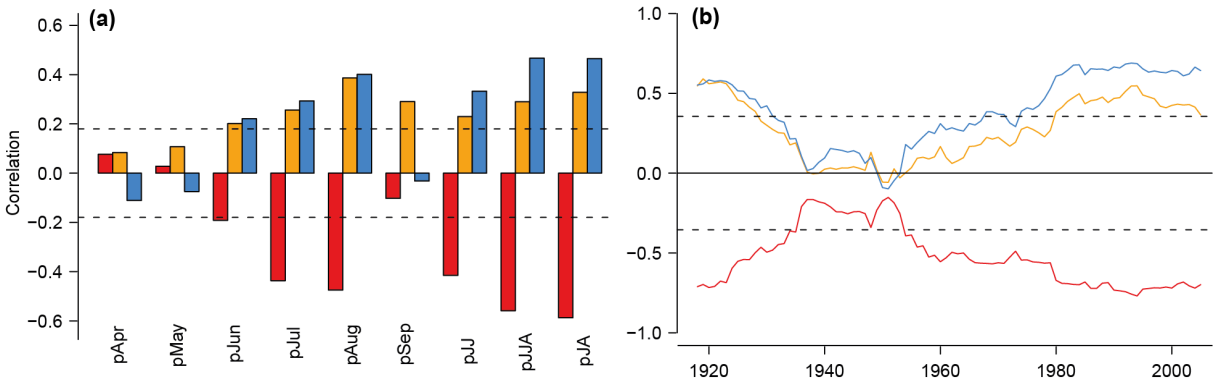

Figure S14. Correlations of the southern composite TRW chronology with previous summer (July–August) Tmax (red), PDSI (orange) and precipitation (blue) for the full period (1902–2020) **(a)** and centered 31-year moving windows **(b)**.

References

Briffa, K. R., Schweingruber, F. H., Jones, P. D., Osborn, T. J., Shiyatov, S. G., & Vaganov, E. A. (1998). Reduced sensitivity of recent tree-growth to temperature at high northern latitudes. *Nature*, *391*(6668), 678–682. https://doi.org/10.1038/35596

Daly, C., Neilson, R. P., & Phillips, D. L. (1994). A Statistical-Topographic Model for Mapping Climatological Precipitation over Mountainous Terrain. *Journal of Applied Meteorology and Climatology*, *33*(2), 140–158. https://doi.org/10.1175/1520-0450(1994)033<0140:ASTMFM>2.0.CO;2

Harris, I., Osborn, T. J., Jones, P., & Lister, D. (2020). Version 4 of the CRU TS monthly high-resolution gridded multivariate climate dataset. *Scientific Data*, *7*(1), 109. https://doi.org/10.1038/s41597-020-0453-3